MOLECULAR AND CELLULAR BIOLOGY, Mar. 2007, p. 1771–1783 Vol. 27, No. 5
0270-7306/07/$08.00+0 doi:10.1128/MCB.00287-06

Role of Cytochrome *c* in Apoptosis: Increased Sensitivity to Tumor Necrosis Factor Alpha Is Associated with Respiratory Defects but Not with Lack of Cytochrome *c* Release[▽]

Uma D. Vempati,[1] Francisca Diaz,[1] Antoni Barrientos,[1] Sonoko Narisawa,[3] Abdul M. Mian,[4] José Luis Millán,[3] Lawrence H. Boise,[2] and Carlos T. Moraes[1,5]*

Departments of Neurology,[1] Microbiology and Immunology,[2] Medical Oncology,[4] and Cell Biology and Anatomy,[5] University of Miami Miller School of Medicine, Miami, Florida, and The Burnham Institute, La Jolla Cancer Research Center, La Jolla, California[3]

Received 15 February 2006/Returned for modification 14 April 2006/Accepted 19 December 2006

Although the role of cytochrome *c* in apoptosis is well established, details of its participation in signaling pathways in vivo are not completely understood. The knockout for the somatic isoform of cytochrome *c* caused embryonic lethality in mice, but derived embryonic fibroblasts were shown to be resistant to apoptosis induced by agents known to trigger the intrinsic apoptotic pathway. In contrast, these cells were reported to be hypersensitive to tumor necrosis factor alpha (TNF-α)-induced apoptosis, which signals through the extrinsic pathway. Surprisingly, we found that this cell line (CRL 2613) respired at close to normal levels because of an aberrant activation of a testis isoform of cytochrome *c*, which, albeit expressed at low levels, was able to replace the somatic isoform for respiration and apoptosis. To produce a bona fide cytochrome *c* knockout, we developed a mouse knockout for both the testis and somatic isoforms of cytochrome *c*. The mouse was made viable by the introduction of a ubiquitously expressed cytochrome *c* transgene flanked by loxP sites. Lung fibroblasts in which the transgene was deleted showed no cytochrome *c* expression, no respiration, and resistance to agents that activate the intrinsic and to a lesser but significant extent also the extrinsic pathways. Comparison of these cells with lines with a defective oxidative phosphorylation system showed that cells with defective respiration have increased sensitivity to TNF-α-induced apoptosis, but this process was still amplified by cytochrome *c*. These studies underscore the importance of oxidative phosphorylation and apoptosome function to both the intrinsic and extrinsic apoptotic pathways.

Cytochrome *c* (Cyt *c*) shuttles electrons from oxidative phosphorylation complex III to complex IV. However, when it is released from mitochondria, it stimulates cell death (15) by interacting with Apaf-1 and recruiting and activating procaspase-9 (27, 46). Apaf-1 and caspase-9 assemble into a multimeric complex known as the apoptosome. Cyt *c* has been shown to catalyze apoptosome assembly but not to be retained in the complex (19, 37, 43).

Much of the current knowledge of the apoptotic pathway involving Cyt *c* came from in vitro assays and more recently from mouse knockouts (KO) (5, 16, 17, 23, 26, 27, 45). Cell culture studies showed that Apaf-1, caspase-9, caspase-3, or *cyt c* KO cells were more resistant to various apoptotic stimuli. The phenotype shared by the mouse KO for Apaf-1, caspase-9, and caspase-3 genes was a severe brain abnormality observed during development. The absence of major defects in other organs suggests that other tissue-specific pathways are involved in the development of these organs. Unfortunately, gene disruption of Apaf-1, caspase-9, and caspase-3 resulted in lethality upon birth or at midgestation. An even more severe phenotype was observed for the *cyt c* KO, which was embryonic lethal (embryos died at 7 to 8 days of gestation [E7 to E8]), probably because of defects in mitochondrial respiration. Embryonic fibroblasts derived from *cyt c* KO embryos were more resistant to some cytotoxic stimuli but surprisingly hypersensitive to tumor necrosis factor alpha (TNF-α) (26). More recently, Hao et al. (17) developed a mouse with a mutated *cyt c* gene knocked in. The mutation (at Lys 72) affected apoptosis but did not appear to have a major effect on respiration. Their studies demonstrated that the apoptotic function of Cyt *c* is required for normal brain development and lymphocyte homeostasis in mice. Their studies with thymocytes from the knockin mice also suggested the existence of an apoptosome-independent caspase activation pathway.

We have previously demonstrated that cells deficient in oxidative phosphorylation (OXPHOS) activity are protected against certain apoptotic stimuli (10). This result was subsequently confirmed by other groups (24, 29, 34). Therefore, despite the demonstration of the importance of Cyt *c* in caspase activation, a role for OXPHOS in this process remains plausible. To further delineate the Cyt *c* OXPHOS-related role in apoptosis, we generated "true" *cyt c* knockout cell lines and compared them to other OXPHOS-deficient cell models.

MATERIALS AND METHODS

Genetically modified mice and derived cell lines. The crosses performed in order to obtain mice with the genotype *cyt* $c_s^{-/-}$ *cyt* $c_t^{-/-}$ Transgene$^{flox/0}$ are described in detail under results. The *cyt* $c_t^{-/-}$ genotype was described in reference 33. The *cyt* $c_S^{-/-}$ mice were obtained from Jackson laboratories (strain name, B6;129-Cycstm1Wlm/J). The floxed *cyt c* transgene was subcloned in the murine Rosa promoter-driven pBroad3 vector (Invivogen). The construct was

* Corresponding author. Mailing address: University of Miami Miller School of Medicine, 1095 NW 14th Terrace, Miami, FL 33136. Phone: (305) 243-5858. Fax: (305) 243-3914. E-mail: cmoraes@med.miami.edu.

▽ Published ahead of print on 8 January 2007.

digested with the PacI restriction enzyme to eliminate the unnecessary plasmid sequence, and the linear fragment was introduced by pronuclear injections into B6/SJLF1 fertilized eggs. The *cyt c* double-KO fibroblast line was derived by mincing lung from a 1-month-old homozygous *cyt* $c_S^{-/-}$ *cyt* $c_t^{-/-}$ mouse harboring the floxed *cyt c* transgene. The transgene was deleted in culture by infection with an adenovirus expressing Cre recombinase (Vector Biolabs).

Mouse genotyping. PCR was performed on tail genomic DNA to obtain mice of the genotype *cyt* $c_s^{-/-}$ *cyt* $c_t^{-/-}$ Transgene$^{flox/0}$. The *cyt* c_s isoform was genotyped by competitive PCR using a forward primer common to both alleles (5′-ACTTGTTTCCAGATTGTCCTC-3′) and *cyt* c^--specific (5′-GCTAAAGC GCATGCTCCAGACTG-3′) and *cyt* c^+-specific (5′-AACCACCAGGAGGCA ACTGT-3′) primers. Primers designed for the detection of wild-type (forward, 5′-CGTTTGGATGCAGAGGAGACTG-3′; reverse, 5′-CTTCTGGAAGAGT GGAGGAAGG-3′) and knockout (forward neo primer, 5′-CCATGGCGATG CCGTCTTGCCG-3′; reverse, 5′-CAAATTGTTCGGCAAATATGCTAC-3′) *cyt* c_t were used to genotype mice. The *cyt c* transgene was detected using primers corresponding to the multiple-cloning sites in the pBroad3 vector (forward, 5′-GTGTG AAACA GGAAG AGAAC-3′; reverse; 5′-ACT TAG GGA ACA AAG GAA CC-3′).

Cell lines. The *cyt* $c_s^{-/-}$ cell line (CRL 2613) was obtained from ATCC. The description states that it was derived from a *cyt c* null mouse embryo at E8/E9 prior to embryonic death. *COX10* knockout mouse embryonic fibroblasts (MEFs) were derived from the skin of *COX10*$^{flox/flox}$ mice (12), cultured, and transfected with a Cre recombinase plasmid construct that deleted the floxed *COX10* gene. As a control, the *COX10* cDNA was reintroduced in *COX10* KO line by lentivirus infection (11). Mouse LM(TK$^-$) cells were obtained from ATCC (CCL 1.3), and the mitochondrial DNA (mtDNA)-less derivative was obtained by ethidium bromide treatment as described previously (9).

Respiration measurements. Cellular respiration was measured by polarography as described by Barrientos et al. (2). The oxygen consumed by cells was measured both before and after addition of the complex III inhibitor, antimycin A, and the subsequent addition of ascorbate and *N*,*N*,*N*′,*N*′-tetramethyl-1,4-phenylenediamine dihydrochloride (TMPD).

Estimation of cytochrome *c* protein. (i) Spectrometric measurement. Cytochrome *c* was estimated as described previously (3). In brief, to a mitochondrial suspension (~10 mg in 500 μl), KCl powder was added to a 670 mM concentration to release the cytochrome *c* and was mixed by gentle pipetting. Then, a buffer containing 50 mM Tris, pH 7.5, and 1% potassium deoxycholate was added to make up the volume to 2 ml and mixed. The suspension was cleared by centrifugation at 40,000 rpm for 15 min at 4°C. To the clear supernatant, sodium cholate was added to a 1% final concentration. Half of the solution was reduced with sodium hydrosulfite and the spectra measured at 500 to 650 nm, while the other half was oxidized with potassium ferricyanide and measured similarly. The differential spectrum was plotted. Cytochromes *c* and c_1 have an absorption peak at 550 nm, cytochrome *b* at 560 nm, and cytochromes *a* and a_3 at 603 nm.

(ii) Reverse-phase HPLC analysis. Cyt *c* was estimated in the mitochondria using a Jupiter C_4 reverse-phase column (Phenomenex) and a high-performance liquid chromatography (HPLC) system (Beckman Instruments) equipped with a UV-VIS detector and Beckman System Gold software as described previously (8, 35). The eluted Cyt *c* was detected at 393 nm, to take advantage of an improved extinction coefficient at that wavelength which results from the presence of trifluoroacetic acid. A linear gradient increasing from 20 to 60% acetonitrile in water was used. Both the 20% and the 60% acetonitrile solutions also contained 100 mM KCl and 0.1% trifluoroacetic acid (vol/vol). Mitochondria (1 mg in a ~20-μl volume) were resuspended with 100 μl of 1% Lubrol WX in water (wt/vol), followed by dilution to 1.0 ml with 150 mM KCl in water, which was buffered at pH 7.4 with 3 mM HEPES. After injection of 250 μg of the acidified (0.1% trifluoroacetic acid) mitochondrial suspension into the HPLC system, the eluted Cyt *c* was detected at 393 nm. Serial dilutions of equine Cyt *c* were made in a buffer containing 0.1 M Mes(Na^+), pH 6.0, 70 μM EDTA, and 25 μM bovine serum albumin and injected into the column to generate a Cyt *c* standard curve.

Cell death assay. Apoptosis was measured by determining chromatin fragmentation using a cell death detection enzyme-linked immunosorbent assay kit from Roche Biochemicals. Cells were treated with staurosporine (1 to 2 μM; Roche Biochemicals) or TNF-α (5 ng/ml; Roche Biochemicals) and cycloheximide (CHX) (Sigma) (1 μg/ml) for 8 to 10 h and subsequently assayed according to the kit protocol. Results were expressed as the average absorbance obtained at 405 to 490 nm for treated and untreated cell lysates. The standard deviation was calculated from the values obtained from three or more independent experiments.

Annexin V–fluorescein isothiocyanate (FITC)–propidium iodide staining. Following treatments with TNF-α (5 ng/ml) and cycloheximide (1 μg/ml) for 8 to 10 h, apoptosis was detected by staining with annexin V-FITC (BioVision) and propidium iodide (Sigma) for 10 min in the dark, followed by flow cytometry.

Measurement of mitochondrial membrane potential. Cells were treated with either dimethyl sulfoxide (solvent) or TNF-α (5 ng/ml) and cycloheximide (1 μg/ml) for 6 to 8 h or with carbonyl cyanide 3-chlorophenylhydrazone (CCCP) (5 μM; Sigma), a protonophore and uncoupler of oxidative phosphorylation, for 15 min, followed by staining with the fluorescent probe tetramethylrhodamine ethyl ester (75 nM; Molecular Probes) and flow cytometric analysis.

Fluorescence caspase assay. The caspase assay was performed based on detection of the cleavage product of a synthetic substrate, which has a 7-amino-4-methylcoumarin (AMC) cleavable moiety. The substrates for caspase-3 and -9 were DEVD-AMC and LEHD-AMC, respectively (BIOMOL research laboratories). Cells were treated with staurosporine and TNF-α plus cycloheximide for 8 to 10 h and subsequently assayed. Results were expressed as the average fluorescence units obtained for treated and untreated cell lysates. The standard deviation was calculated from the values obtained from three or more independent experiments.

Immunostaining. Live cells were stained with Mitotracker-red (200 nM; Molecular Probes) and subsequently fixed and permeabilized in 4% paraformaldehyde and ice-cold methanol, respectively. Then, cells were incubated with a primary antibody against Cyt *c* (BD Biosciences) and subsequently with a secondary antibody tagged with fluorescent Alexa-fluor (Molecular Probes) and visualized by confocal microscopy. An anti-Cyt *c* testis isoform was prepared against a synthetic peptide as described previously (33).

Restriction fragment length polymorphism of testis and somatic *cyt c* cDNAs. RNAs isolated from cell lines and mouse testes were used as templates for cDNA synthesis. Oligonucleotide primers perfectly matching both the somatic and testis *cyt c* cDNAs (forward, 5′-GGCAAGAAGATATTTGTTCAGAA-3′; reverse, 5′-GCTTCTCCAAATAGTCCATCA-3′) were used to amplify the cDNA templates. The amplicon was digested with DdeI or HinfI, both of which can differentiate the somatic and testis *cyt c* isoforms, and the products were resolved by native polyacrylamide gel electrophoresis.

Isolation of RNA and reverse transcription. Total RNA was isolated from cells and mouse tissues using the Trizol reagent (Invitrogen, CA) as per the manufacturer's recommendation. Reverse transcription was done using random hexamers on 5 μg of RNA with Superscript II reverse transcriptase (Invitrogen).

Isolation of mitochondria. Mitochondria were prepared by the nitrogen cavitation method as described by Gottlieb and Adachi (14) with some modifications. In brief, cells were washed in 10 ml of the ice-cold buffer A (100 mM sucrose, 1 mm EGTA, 20 mM morpholinepropanesulfonic acid, pH 7.4) and centrifuged at 1,500 × *g* to pellet. Cells (~1 ml pellet) were resuspended in 5 ml of hypotonic ice-cold buffer B (buffer A plus 10 mM Triethanolamine, 5% Percoll, and protease inhibitor cocktail [complete; Roche Biochemicals]) and subjected to nitrogen cavitation at 500 lb/in^2 for 30 min. The mix of broken cells was centrifuged twice at 500 × *g* and the final supernatant centrifuged at 12,000 × *g*. The pellet was used as a crude mitochondrial preparation.

Western blots. Cell lysates were prepared as described for detection of caspases. In brief, cells were lysed in buffer (150 mM NaCl, 1% NP-40, 0.5% sodium deoxycholate, 0.1% sodium dodecyl sulfate, 50 mM Tris, pH 8.0, supplemented with Complete protease inhibitor cocktail [Roche Biochemicals]), and protein concentrations were determined using the D_C kit (Bio-Rad Laboratories). Cell lysates and mitochondrial preparation were resolved on precast sodium dodecyl sulfate-polyacrylamide gels, transferred onto a polyvinylidene difluoride membrane, and hybridized with the antibodies raised against Cyt c_s, Cyt c_t (33), VDAC (Molecular Probes, OR), activated caspase-3 (Cell Signaling), procaspase-9 (MBL Biological laboratories), Bid (R&D Systems), TNFR-1 (Stressgen), glyceraldehyde-3-phosphate dehydrogenase (Ambion, TX), and β-tubulin (Sigma).

Measurement of cytochrome *c* release. Cytochrome *c* release was estimated by Western analysis of the mitochondrial and cytosolic fractions prepared by the method described in reference 42. In brief, cells were harvested in isotonic mitochondrial buffer (MB) (210 mM mannitol, 70 mM sucrose, 1 mM EDTA, 10 mM HEPES [pH 7.5]) supplemented with complete protease inhibitor cocktail (Roche Biochemicals). The cells were broken by six passages through a 25G1 0.5-by 25-mm needle, and the suspension was centrifuged at 2,000 × *g* in a centrifuge at 4°C. This procedure was repeated twice, and supernatants from each step were pooled before being subjected to centrifugation at 13,000 × *g* at 4°C for 10 min. The supernatant was further centrifuged at 100,000 × *g* for 10 min at 4°C to yield the light membrane pellet (not analyzed) and the final soluble fraction (S100). The heavy membrane material was pooled and resuspended in MB-EGTA (MB with 0.5 mM EGTA instead of EDTA) and centrifuged at 500 × *g* for 3 min at 4°C to eliminate residual nuclei. The resulting supernatant was centrifuged at 13,000 ×

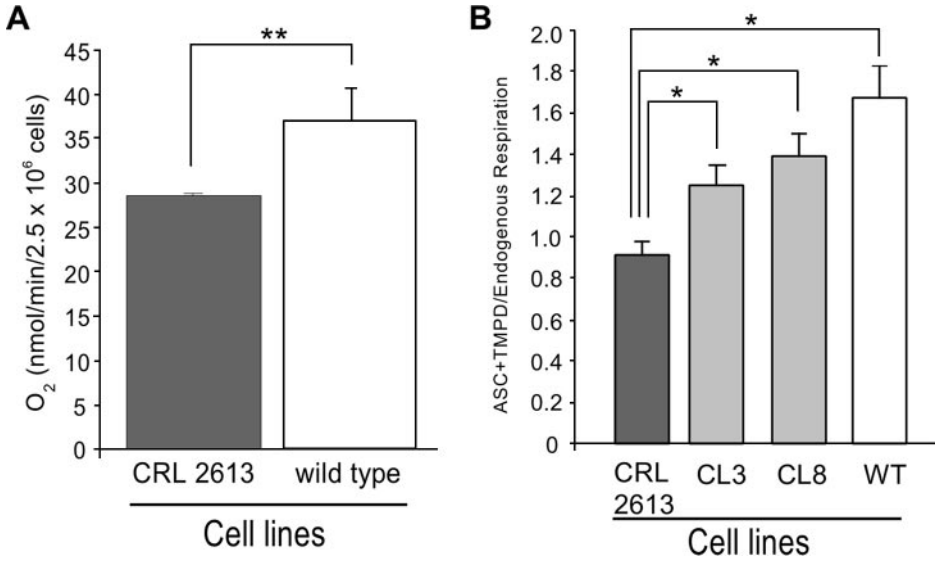

FIG. 1. Mouse embryonic fibroblasts with disrupted *cyt c* (somatic) alleles show mitochondrial respiration. Panel A, CRL 2613 and control MEFs were analyzed for KCN-sensitive oxygen consumption by intact cells. Panel B, somatic *cyt c* cDNA was reintroduced in the CRL 2613 line, and clones expressing the cDNA were obtained (clones CL3 and CL8). All cell lines were also analyzed for the ratio of ascorbate-TMPD respiration (where electrons are donated directly to Cyt *c*) to endogenous respiration (starting at complexes I and II). $n \geq 3$; *, $P < 0.005$; **, $P < 0.05$.

g for 10 min at 4°C to further purify the mitochondrial fraction. The protein concentration was estimated using the D_C kit (Bio-Rad Laboratories).

RESULTS

A mouse embryonic fibroblast cell line derived from a mouse with *cyt c* (somatic) knocked out expresses the *cyt c* (testis) gene. To better understand the in vivo contribution of Cyt *c* to apoptosis, we obtained a MEF cell line with the somatic form of the *cyt c* gene knocked out (line CRL 2613 from ATCC). This cell line was derived by Li and colleagues (26) as described in Methods. To assure that the cell line had no Cyt *c*, we performed whole-cell respiration studies. Unexpectedly, CRL 2613 respiration was only 25% lower than that of a control MEF, and this respiration was completely inhibited by KCN (Fig. 1A), indicating that it was taking place in the mitochondrial respiratory chain. In addition, ascorbate-TMPD (AT), which donates electrons directly to Cyt *c*, also promoted KCN-sensitive respiration. The ratio of AT respiration to total respiration (from endogenous substrates) was moderately decreased compared to that for a control cell line (Fig. 1B). As additional controls, we reintroduced the somatic isoform of *cyt c* in the CRL 2613 cell line (CL3 and CL8). The gene reintroduced was a somatic mouse *cyt c* cDNA cloned in the pBROAD3 expression vector (see Fig. 5B). The AT/endogenous respiration ratio was also higher for these clones than for CRL 2613 (Fig. 1B). These initial observations raised the possibility that CRL 2613 had a functional Cyt *c* pool, albeit reduced in size.

Immunocytochemistry showed a marked reduction in Cyt *c* levels in the CRL 2613 line (Fig. 2A). Cyt *c* levels were increased by the introduction of the *cyt c* cDNA by stable transfection (Fig. 2A). These observations were confirmed by Western blotting using a monoclonal antibody against Cyt *c* (Fig. 2C, top). Because mice contain a testis-specific *cyt c* isoform (*cyt* c_t), we investigated if the CRL 2613 cells expressed this tissue-specific *cyt c* isoform. RNA was isolated from the different cell lines and a fragment amplified by reverse transcription (RT)-PCR. This fragment was chosen because of the presence of a diagnostic restriction fragment length polymorphism that could distinguish the somatic and testis isoforms. This experiment clearly showed that although control MEFs did not express the testis isoform, the CRL 2613 line did (Fig. 2B). Western blotting with an antibody raised against the testis isoform confirmed that CRL 2613 had an active Cyt *c* testis isoform (Fig. 2C, bottom). Although the antibodies against the testis and somatic isoforms showed a small level of cross-reactivity, the introduction of the somatic *cyt c* cDNA into CRL 2613 appeared to downregulate the testis isoform (CL3 and CL8 in Fig. 2C). Next, we determined the steady-state levels of Cyt *c* in this cell line. By cytochrome spectra, we determined that the levels of Cyt *c* were decreased in CRL 2613, but because the Cyt *c* peak overlaps with the Cyt c_1 (a subunit of complex III) peak at 550 nm, we could not perform a precise quantification (Fig. 3A). Therefore, we determined the levels of Cyt *c* by reverse-phase HPLC as described in Methods. This experiment showed that in CRL 2613, Cyt *c* (testis isoform) levels were present at 29% of the levels of the somatic form in a control MEF cell line (Fig. 3B).

Testis Cyt *c* can promote apoptosis. We evaluated the sensitivity of CRL 2613 and the clones with reintroduced somatic *cyt c* (CL3 and CL8) to different apoptosis triggers. Inducers of both the intrinsic (staurosporine) and extrinsic (TNF-α) pathways caused chromatin fragmentation (Fig. 4A) and caspase-3 (Fig. 4B, C, and F) and -9 (Fig. 4D, E, and G) activation. We observed a similar result after serum starvation (not shown). These findings suggest that a two-thirds reduction in Cyt *c* levels does not have a major influence in the susceptibility to apoptosis. By reintroducing a somatic *cyt c* cDNA in this cell

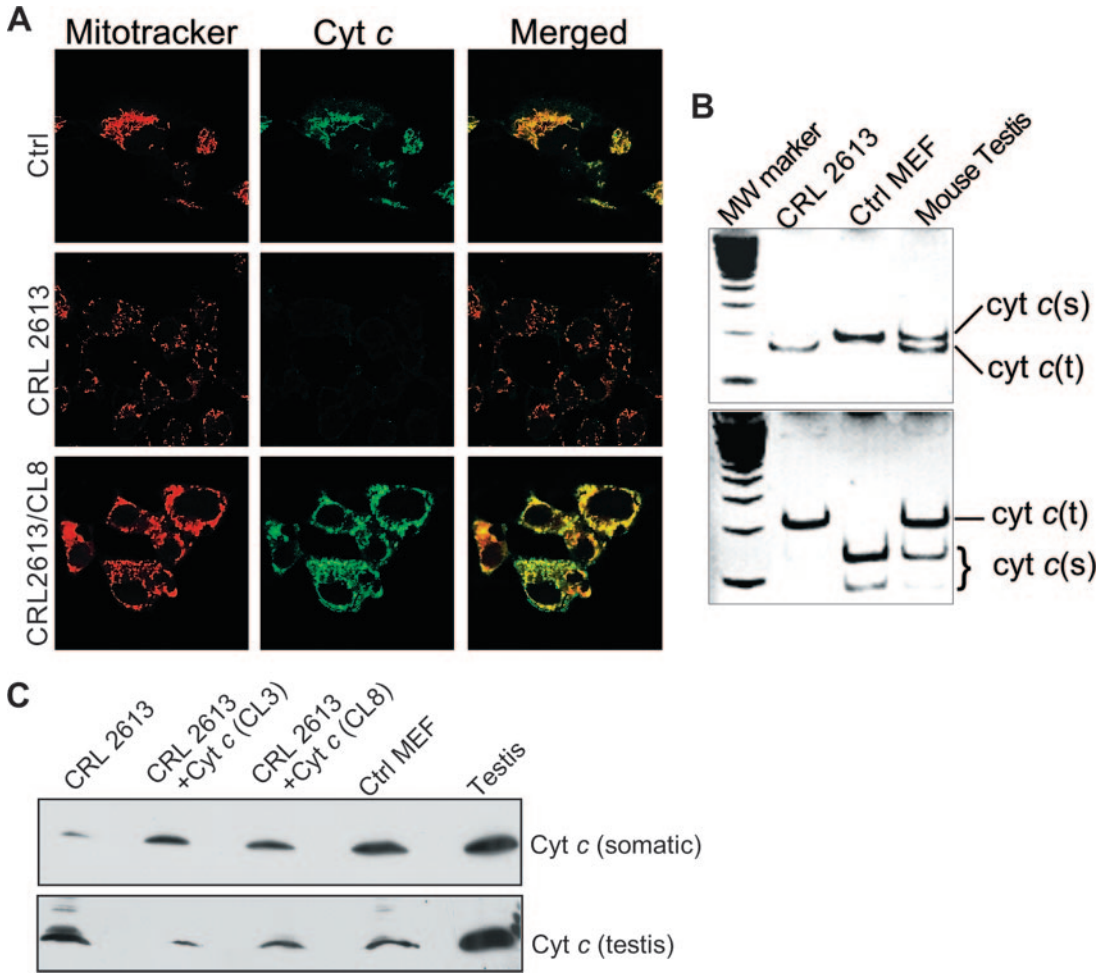

FIG. 2. Mouse embryonic fibroblasts with disrupted *cyt c* (somatic) alleles have an active testis isoform of *cyt c*. Panel A, CRL 2613, its derivative with a reintroduced somatic cDNA (CL8), and a wild-type MEF were immunostained for Cyt *c* (middle panels) and costained with Mitotracker-Red (left panels). CRL 2613 showed a marked decrease in Cyt *c*-immunoreactive material. Panel B, RT-PCR followed by restriction fragment length polymorphism analysis (DdeI, top; HinfI, bottom) revealed that CRL 2613 expresses an active testis isoform of Cyt *c*. Panel C, using an antibody raised against the testis isoform of Cyt *c*, we confirmed the presence of this isoform in CRL 2613 cells. The samples were also probed with a Cyt *c* monoclonal antibody raised against the somatic form.

line, we did not observe a marked increase in apoptosis. Although activation of caspase-3 was higher in some clones (e.g., CL8), the overall cell death was similar to that for the parental CRL 2613 (Fig. 4A). Interestingly, CRL 2613 as well as its derivative CL3 and CL8 lines showed less activation of caspase-3 and -9 than an unrelated MEF control, suggesting that the CRL 2613 nuclear background has undergone additional adaptations (Fig. 4B and D).

The creation of a bona fide *cyt c* knockout cell line. Based on the observations described above, we decided to create a cell line that would be a true *cyt c* knockout. To do so, we crossed mice harboring a heterozygous somatic *cyt c* KO allele (*cyt* $c_s^{+/-}$) with mice harboring a homozygous testis *cyt c* KO allele (*cyt* $c_t^{-/-}$). The *cyt c* testis KO was previously characterized, and besides reduction in male fertility and early testicular atrophy, no other major abnormal phenotype was observed (33). Spermatogonia, diploid germ cells, express only Cyt c_s. From the preleptotene to the pachytene stages of meiotic prophase, expression of Cyt c_s decreases while levels of Cyt c_t increase (18). Cyt c_t is the sole Cyt *c* expressed in postmeiotic male germ cells, including mature spermatozoa. Therefore, we used homozygous *cyt* $c_t^{-/-}$ females for the crosses (Fig. 5A). To both expand the possible cell types to be studied and avoid the difficult procedure of isolating MEF lines from E8 embryos (the stage where *cyt* $c_s^{-/-}$ embryos die), we chose to rescue the embryonic lethal phenotype by introducing a ubiquitously expressed somatic *cyt c* transgene flanked by loxP sites (Fig. 5B). Expression of the transgene in founder transgenic lines was confirmed by RT-PCR of heart and brain RNA. Because the transgene had an intron spanning the amplicon, we observed additional specific bands in the RT-PCR, which likely correspond to the amplification from differentially spliced transcripts and formation of heteroduplexes (Fig. 5C). Crosses of one of the transgenic animals (line 4395) with the *cyt* $c_t^{-/-}$ *cyt* $c_s^{+/-}$ animals gave rise to F_1 mice that when backcrossed produced mice with the *cyt* $c_t^{-/-}$ *cyt* $c_s^{-/-}$ *cyt* $c^{flox/o}$ genotype, demonstrating that the transgene was able to rescue the embryonic lethal phenotype of the *cyt* c_s KO (Fig. 5D). Lung

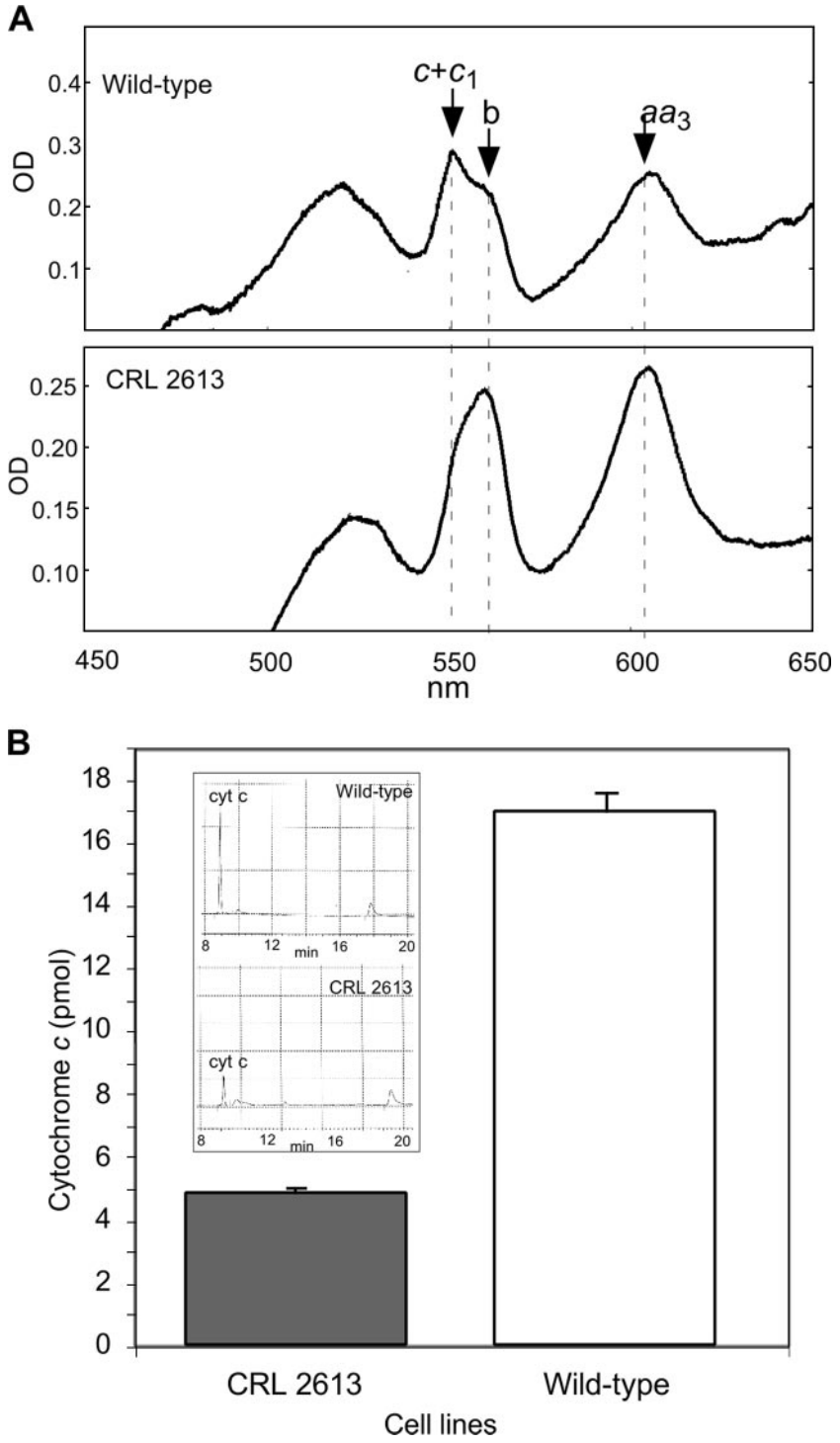

FIG. 3. Levels of Cyt *c* in the mouse embryonic fibroblasts with disrupted *cyt c* (somatic) alleles are markedly reduced. Panel A, spectrometric measurement. We isolated mitochondria and extracted cytochromes from CRL 2613 and a MEF control. The cytochrome spectra (500 to 650 nm) showed a marked reduction in the peak, corresponding to *c*-type cytochromes (at 550 nm). Cytochromes *c* and c_1 have an absorption peak at 550 nm, cytochrome *b* at 560 nm, and cytochromes *a* and a_3 at 603 nm. Panel B, reverse-phase HPLC analysis. The levels of total Cyt *c* in CRL 2613 cells were determined by HPLC as described in Methods. This quantitative analysis showed that CRL 2613 had only 29% of the Cyt *c* levels found in the control MEF cells. The inset in panel B shows representative HPLC profiles.

fibroblasts (LF) from these animals were cultured and the transgenic *cyt c* cDNA deleted ex vivo by an adenovirus preparation expressing the Cre recombinase (Fig. 5A). Immunocytochemical examination of the Ad-Cre-treated cells showed that approximately 30% of the cells were negative for Cyt *c* (Fig. 6, upper row). Because increasing the amounts of adenovirus did not alter this ratio significantly, we isolated individual clones by serial dilution and screened them for the

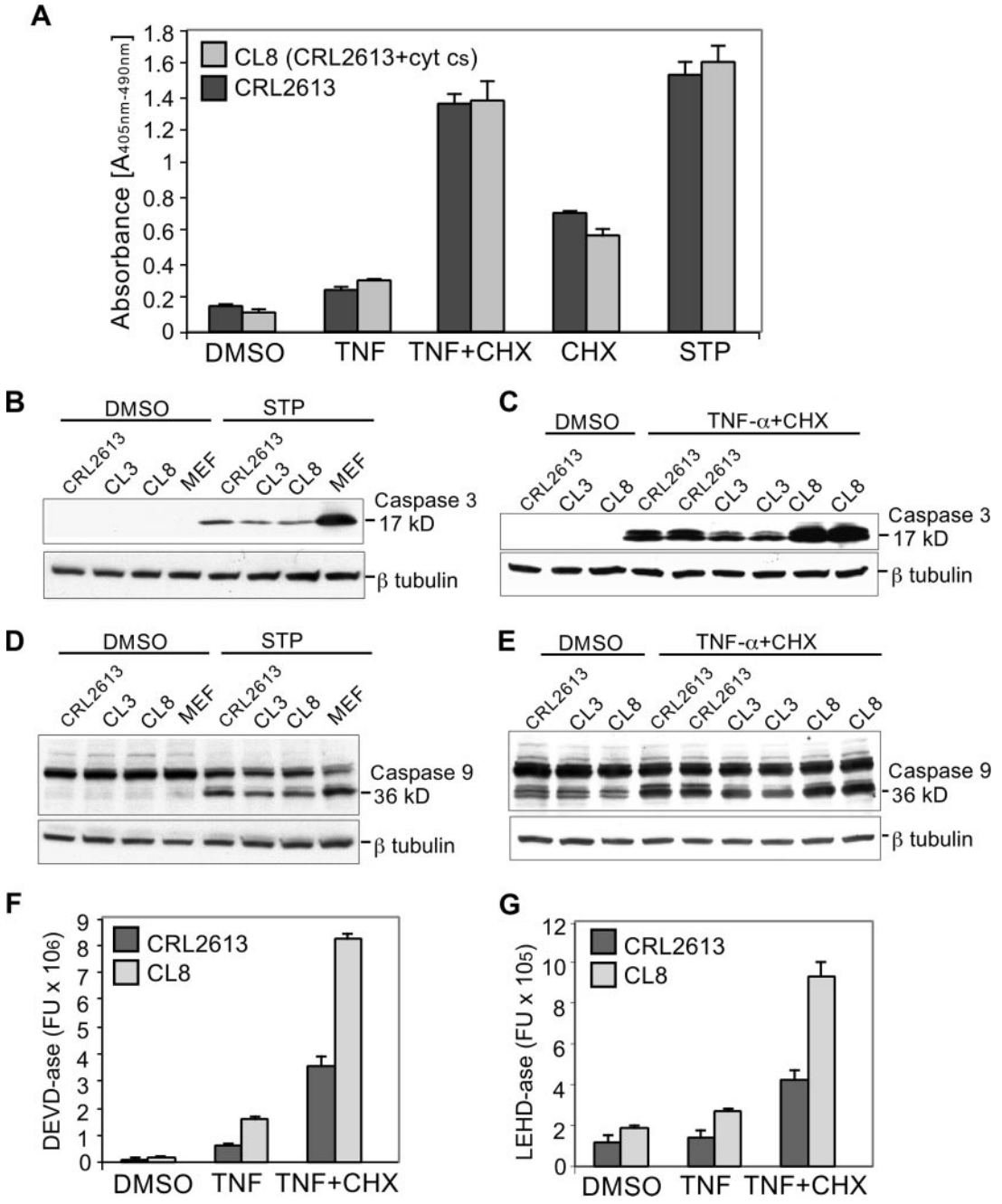

FIG. 4. Effect of partial cytochrome *c* depletion on apoptosis. Cells were treated with the carrier dimethyl sulfoxide (DMSO) and 5 ng/ml TNF-α with or without the addition of 1 μg/ml CHX, 1 μg/ml CHX alone, or 2 μM staurosporine (STP). Panel A, Apoptosis was measured by determining the chromatin fragmentation in CRL 2613 and clone CL8. Western blots of cell lysates prepared from dimethyl sulfoxide and staurosporine treated (panels B and D) or TNF-α–CHX treated (panels C and E) were probed with antibodies against caspase-3 and -9. The active forms of caspase-3 and -9 were detected at ~17 kDa and 36 kDa, respectively. Tubulin antibody was used as a loading control. Fluorescence caspase assays based on detection of the cleavage product of synthetic substrates (DEVD and LEHD), which have 7-amino-4-methylcoumarin (AMC) at the C-terminal end, were also employed (panels F and G). Caspase-3 and -9 specifically cleave after the aspartate residue in the DEVD or the LEHD peptide sequence, respectively. Results represent averages of data obtained from three or more independent experiments.

presence of Cyt *c*. As expected, some of the isolated clones had no detectable Cyt *c* as determined by immunocytochemistry (Fig. 6, lower rows). Clones LF-CL3, LF-CL4, and LF-CL7, which lacked all *cyt c* alleles, were used in subsequent experiments. These clones did not respire (Fig. 5E), and Western blots using both the commercial anti-Cyt *c* (inset in Fig. 5E) and the anti-testis Cyt *c* (not shown) antibodies could not detect Cyt *c* in these clones.

***Cyt c* null cells are resistant to intrinsic and extrinsic apoptotic stimuli.** The *cyt c* double KO clones showed a marked

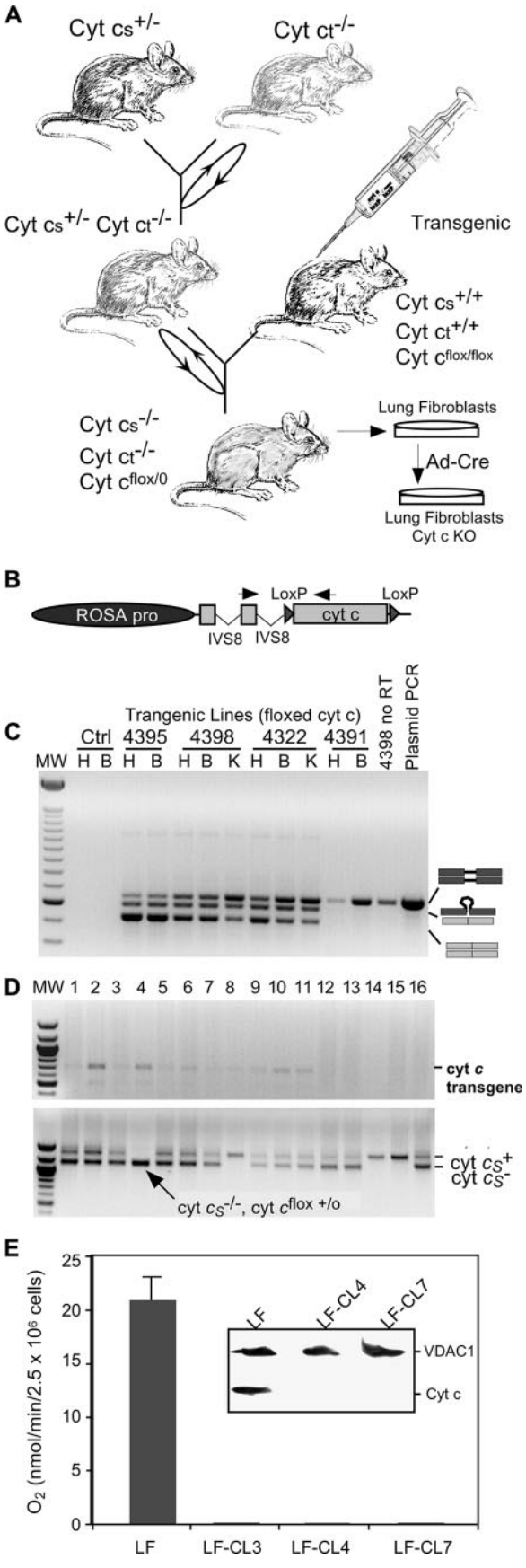

FIG. 5. Development of a null *cyt c* cell model. Panel A illustrates the general approach used to develop a *cyt c* knockout cell line. We crossed mice with testis *cyt c* knockout with the somatic *cyt c* knockout. Backcrosses allowed the isolation of mice with appropriate alleles that were further crossed with a transgenic mouse harboring a loxP-flanked *cyt c* transgene. The structure of the transgene is depicted in panel B. The transgenic lines were screened by RT-PCR specific for the transgene. Because the PCR spans an intron, we detected different mRNA forms, as illustrated in panel C. Panel D shows the PCR analysis of a cross where animals homozygous for the somatic *cyt c* were obtained, demonstrating the ability of the transgene to rescue the embryonic lethal phenotype. Panel E, after the establishment of lung fibroblast (LF) cultures, clones lacking Cyt *c* were isolated (e.g., LF-CL4 and LF-CL7) by adenovirus Cre infection. Clones with the *cyt c* transgene deleted did not consume oxygen that is KCN inhibitable. The inset on panel E shows a Western blot probed with anti-Cyt *c* and anti-VDAC1 antibodies. The latter antibody was used for the detection of a control mitochondrial protein. The KO clones had undetectable levels of Cyt *c* in this Western analysis.

resistance to staurosporine-induced cell death, as measured by chromatin fragmentation and caspase-3 and -9 activation (Fig. 7A and B). In contrast to what has been reported for the *cyt* c_s KO MEFs (26), these cells were also less sensitive to TNF-α-induced cell death (Fig. 7A and C to E), even though a certain level of caspase-3 and -9 processing was observed (Fig. 7C to E). The reduced, but still detectable caspase-3 activation after TNF-α treatment in the KO clones indicated that, as expected, caspase-3 can be activated by caspase-8 (1, 38). These results were essentially identical for three independent clones (Fig. 7).

Defects in oxidative phosphorylation increase sensitivity to TNF-α. In order to compare the consequences of Cyt *c* depletion with those caused by an OXPHOS deficiency, we treated the *cyt c* KO lung fibroblasts, as well as two other mouse cell lines defective in OXPHOS, with apoptotic inducers. As a model of cytochrome oxidase (COX) deficiency, we used a cell line with a deletion in the *COX10* gene, which codes for a factor involved in the maturation of COX. The production of the floxed *COX10* allele has been described previously (12), and the cell line has been extensively characterized (11). In brief, the deletion of the gene in culture was done by expression of the *Cre* recombinase. The *COX10* KO cells cannot mature COX I, which becomes functionless and highly unstable (Fig. 8A). As controls, we used a *COX10* KO line in which the *COX10* cDNA was reintroduced. We also used a [*rho*^{0}] derivative (i.e., mtDNA-less) of the LM(TK$^-$) cell line previously produced and characterized (9). The [*rho*^{0}] cells lack all mtDNA-encoded subunits of the OXPHOS complexes, including COX I. Interestingly, the *cyt c* KO cells appear to have very low levels of COX I (Fig. 8A).

All of these cell lines were characterized for OXPHOS function by measuring their KCN-sensitive oxygen consumption. As expected, the [*rho*^{0}], *COX10* KO, and *cyt c* KO lines did not respire (Fig. 8B). *COX10* knockout and [*rho*^{0}] cells underwent staurosporine-induced apoptosis at levels that were lower than those for the wild-type cells (Fig. 8C), confirming previous observations (10). However, this protection was not as robust as the protection conferred by not having Cyt *c*. In contrast, all the OXPHOS-deficient cells (with the exception of the *cyt c* KO) showed increased sensitivity to TNF-α-induced cell death (Fig. 8C). The OXPHOS-deficient cell lines had a mildly de-

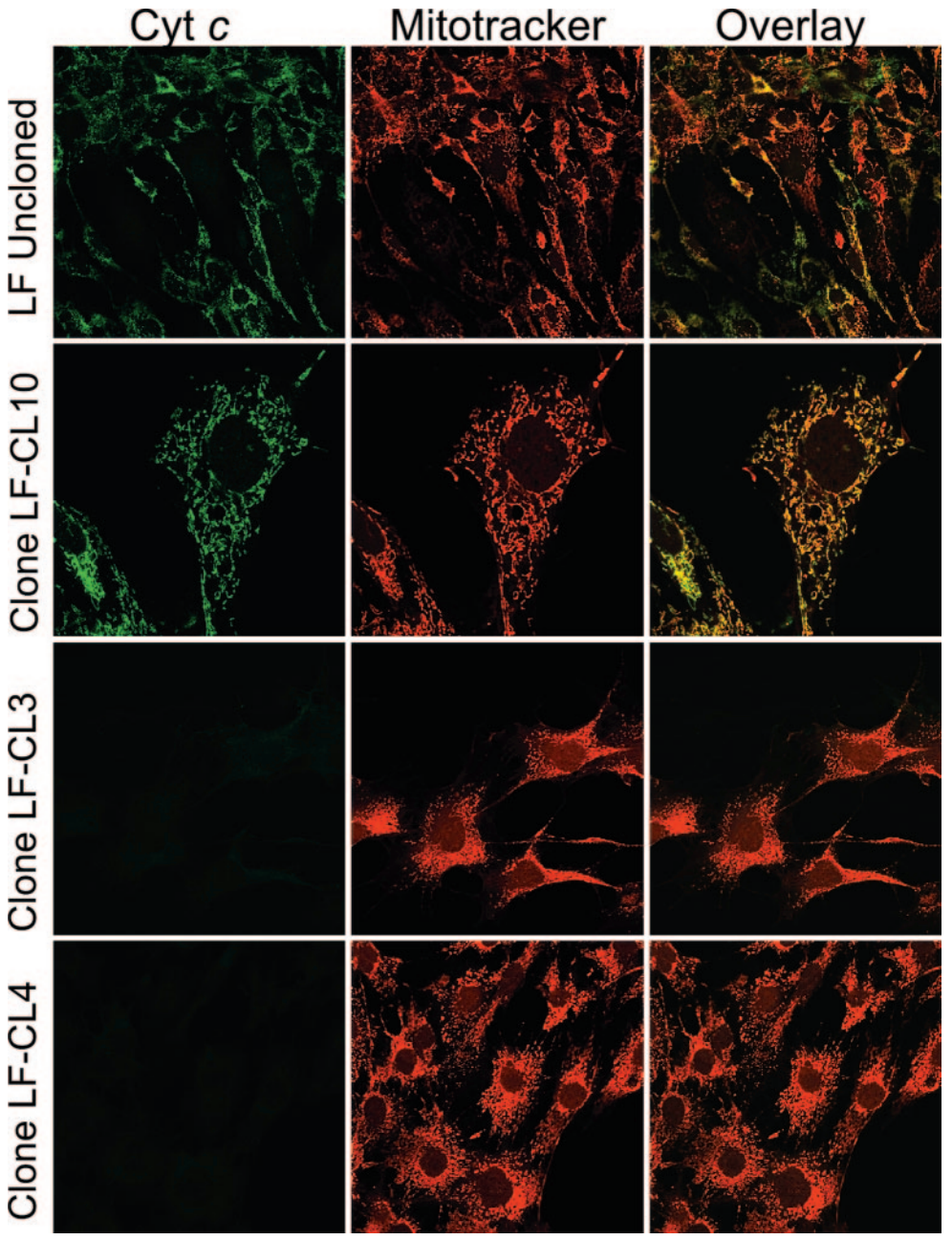

FIG. 6. Immunocytochemical characterization of fibroblast clones without Cyt *c*. The figure illustrates the *cyt c* transgene deletion after adenovirus Cre infection of lung fibroblasts (LF uncloned). After cloning the mixed populations, we obtained pure clones devoid of Cyt *c* (e.g., LF-CL3 and LF-CL4).

creased mitochondrial membrane potential ($\Delta\psi m$). The $\Delta\psi m$ in OXPHOS-deficient cells is maintained by the reverse proton flow mediated by the adenine nucleotide translocator and F1 ATPase function (4). Treatment with TNF-α (5 ng/ml) and cycloheximide (1 μg/ml) for 8 h resulted in a slight reduction in $\Delta\psi m$, and this effect was similar in both OXPHOS-competent and OXPHOS-deficient cell lines (Fig. 8D). Similar results were obtained for the *COX10* KO cells (not shown). Treatment with CCCP resulted in a reduction in $\Delta\psi m$ that was more pronounced in the OXPHOS-deficient cells (Fig. 8D).

To further confirm the TNF-α hypersensitivity of OXPHOS-deficient cells, we tested the sensitivity of human [rho^0] cells to TNF-α. This osteosarcoma-derived [rho^0] cell line (143Bρ^0) was also more sensitive to TNF-α than the control with the same nuclear background but containing mtDNA (Fig. 9A). These same cells overexpressing Bcl-xL were protected from TNF-α-induced apoptosis (Fig. 9A), supporting a mitochondrial role in TNF-α-induced apoptosis.

We also measured the steady-state levels of the TNF-α receptor 1 (TNFR1) (Fig. 9B). We found that upon TNF-α treatment, the levels of TNFR1 increased, probably due to internalization and protection from degradation. The process-

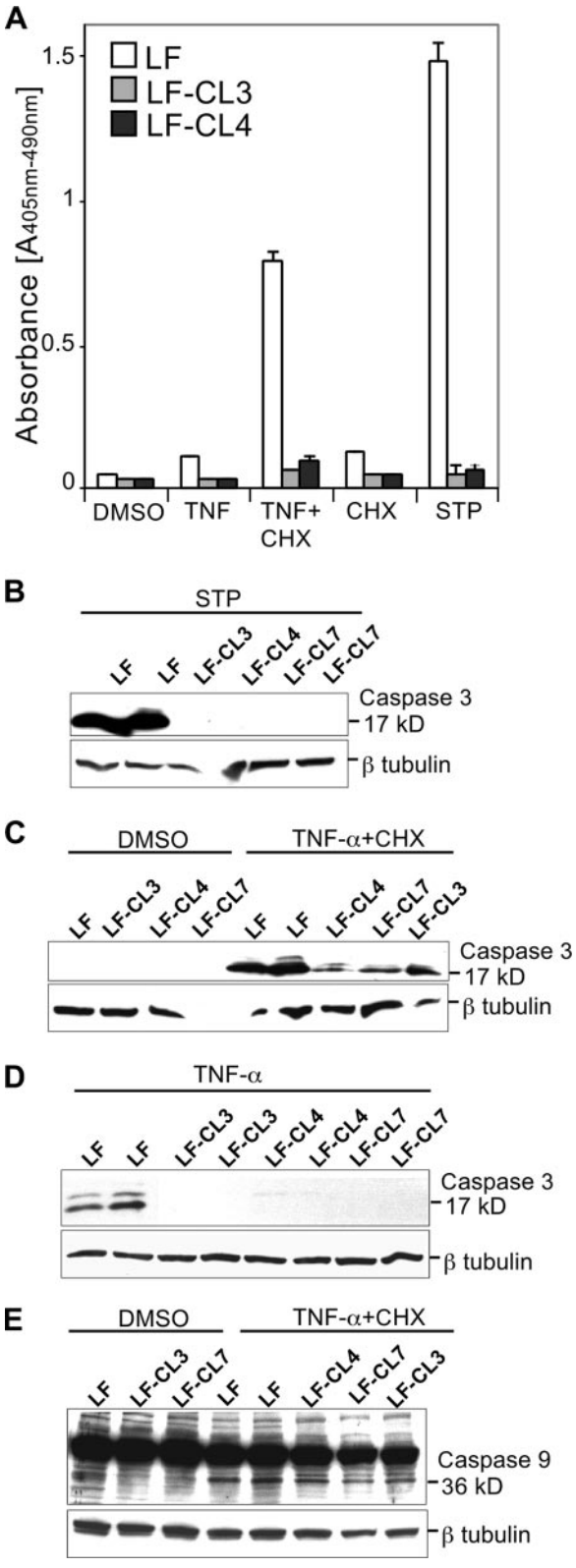

FIG. 7. *cyt c* knockout fibroblasts have reduced sensitivity to TNF-α-induced apoptosis. Cells were treated with the carrier dimethyl sulfoxide (DMSO), 2 μM staurosporine (STP), or 5 ng/ml TNF-α with or without the addition of 1 μg/ml CHX. Panel A, apoptosis was measured by determining the chromatin fragmentation in lung fibroblasts (LF) and derivative *cyt c* KO clones (LF-CL3 and LF-CL4). Panels B to E, Western blots of cell lysates prepared from staurosporine-treated (B) or dimethyl sulfoxide- or TNF-α–CHX-treated (C and E) cell extracts or cell extracts treated with TNF-α alone (D) using antibodies against caspase-3 (B to D) and -9 (E). The active forms of caspase-3 and -9 were detected at ~17 kDa and 36 kDa, respectively. Tubulin antibody was used as a loading control.

ing of Bid to tBid, which is initiated by TNF-α signaling and mediated by caspase-8, was more cell type dependent and could not explain the increased activation of caspase-3 and -9 in the OXPHOS-deficient cells (Fig. 9B). We also analyzed the release of Cyt *c* in the two OXPHOS-deficient mouse cell lines containing Cyt *c*, namely, LM(TK$^-$)ρ^0 and the *COX10* KO, upon TNF-α–CHX treatment (Fig. 9C). The LM(TK$^-$)ρ^0 line showed increased Cyt *c* release compared to that for LM(TK$^-$). The *COX10* KO line showed only a slightly greater increase in Cyt *c* release than the control. Taken together, these results suggest that a combination of metabolic changes in OXPHOS-deficient cells may contribute to the increased sensitivity to TNF-α.

DISCUSSION

The role of cytochrome *c* in apoptosis is now well established, yet most evidence on a direct participation came from in vitro studies (20, 22, 27, 28). The first direct in vivo evidence that Cyt *c* is critical for the apoptotic process came from a mouse knockout study (26). Because Cyt *c* is required for mitochondrial respiration, mice homozygous for the null allele displayed an embryonic lethal phenotype. Nonetheless, the authors were able to derive MEFs from E7 to E9 embryos, which showed resistance to several apoptosis inducers but hypersensitivity to TNF-α, which stimulates the extrinsic pathway for caspase activation (26). More recently, a knockin model with a mutated lysine 72 of Cyt *c*, which was known to affect its role in apoptosis (22), was produced. Respiration was preserved with the mutant Cyt *c*, allowing some homozygous mutant mice to develop to term. However, these mice had severe brain abnormalities, which were ascribed to defective apoptosis during central nervous system development, and died soon after birth (17).

The availability of cell lines with *cyt c* mutant alleles allows in-depth investigations of the role of this molecule in different aspects of cell death. Therefore, we obtained the ATCC-distributed MEF cell line derived by Li and colleagues (26) to perform such studies. However, we found that these cells had an activated testis isoform of Cyt *c*. It is not clear at which point the activation of the testis isoform occurred. We found that immunological detection of Cyt *c* in this cell line was markedly reduced (estimated as an approximately two-thirds reduction from control levels). These reduced levels of Cyt *c* were sufficient for 75% of normal cell respiration or ascorbate-TMPD-mediated respiration. They were also sufficient to confer sensitivity to apoptotic inducers. Although the sequence of the testis isoform is 87% identical to that of the somatic form at the amino acid levels, we provided the first in vivo evidence that the testis isoform can work in these two biological processes in the context of a somatic cell.

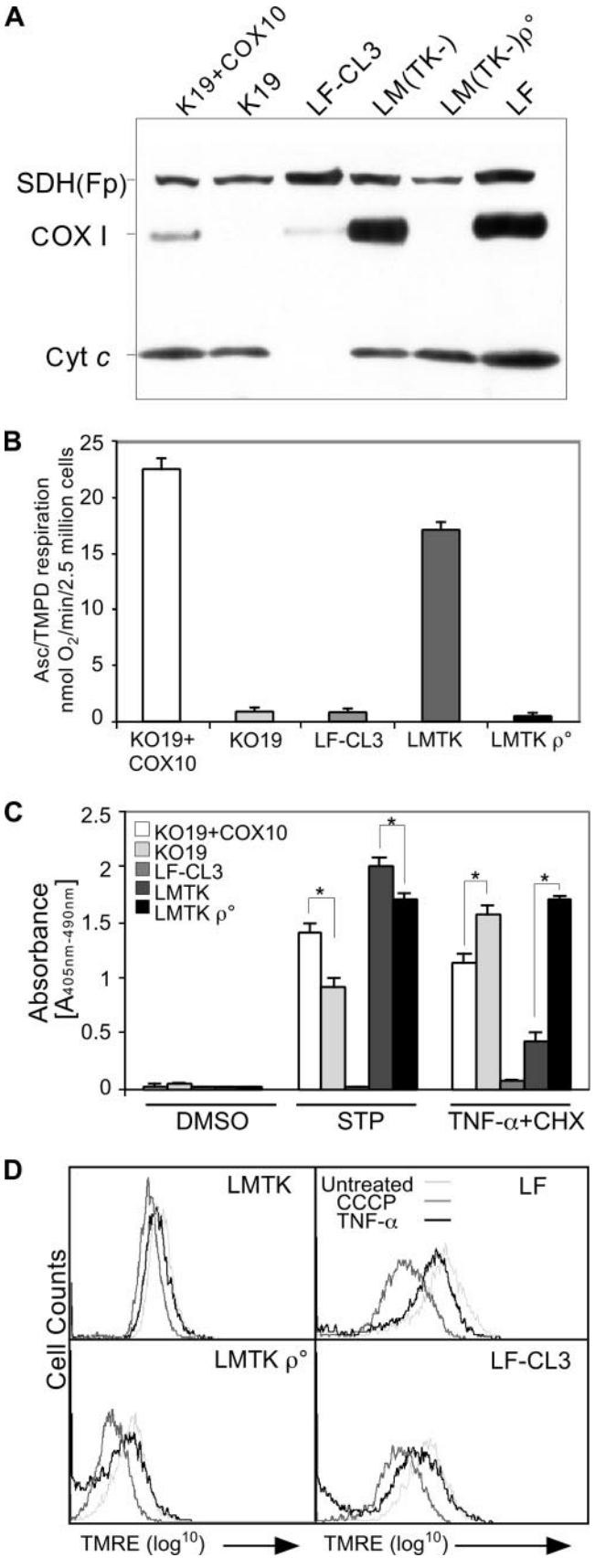

To produce bona fide *cyt c* KO cells, we took advantage of existing *cyt c* somatic and testis knockout mice and a newly created conditional transgenic model to prepare lung fibroblasts devoid of Cyt *c*. These double knockout cells were resistant to inducers of both the intrinsic and extrinsic apoptosis pathways. It is unclear why the MEF cells derived by Li and colleagues showed TNF-α hypersensitivity (26). Based on our finding, we could speculate that if the testis isoform of *cyt c* was expressed at very low levels in early passages, sufficient to stimulate apoptosis but not to support normal respiration, it would be easier to explain the hypersensitivity to TNF-α (see below). However, our results suggest that in the complete absence of Cyt *c*, apoptosis triggered by TNF-α is impaired. These results are consistent with a role for the mitochondrial pathway in death receptor signaling (13, 36, 39, 41). It is well established that TNF-α leads to caspase-8-dependent Bid cleavage to truncated Bid (tBid), which translocates to mitochondria (25, 30, 32). tBid stimulates Bax oligomerization, thereby promoting the release of apoptogenic factors, such as Cyt *c*, from the mitochondria (21, 30, 44). Therefore, the reduced TNF-α-induced apoptosis in *cyt c* null cells fits the current model. Moreover, Bcl-xL overexpression was able to protect both a respiration-competent and -deficient cell line against TNF-α, supporting an important role for the mitochondria in amplifying the death signal, as reported previously (40).

Two additional important conclusions were derived from our studies with respiratory mutants. (i) The protective effect of *cyt c* removal is not related solely to the lack of respiration. COX-deficient or [rho^0] cells showed some protection against staurosporine, but this effect was much weaker than the one observed in cells without Cyt *c*. These results support the recent observations with a knockin *cyt c* mouse lacking apoptotic function but retaining a respiratory capacity (17). This discrimination is important, because OXPHOS defects have been associated with decreased susceptibility to some apoptotic stimuli (10, 24, 34), results that were confirmed here. (ii) OXPHOS-defective cells were more sensitive to TNF-α-induced apoptosis. The respiratory mutant cell lines showed increased sensitivity to TNF-α-induced apoptosis compared to

FIG. 8. Effect of Cyt *c* and OXPHOS deficiency on apoptosis. Western blots in panel A show the absence of components that are required for cell respiration, namely, COX I in K19 and LM(TK^-)ρ° cells and Cyt *c* in the LF-CL3 cells. SDH(Fp) is a subunit of complex II, which is nuclearly encoded. Panel B shows oxygen consumption by the different cell lines after addition of ascorbate-TMPD, which donates electrons to Cyt *c*. Panel C, cells were treated with the carrier dimethyl sulfoxide (DMSO), 1 μM staurosporine (STP), or 5 ng/ml TNF-α with the addition of 1 μg/ml CHX. Apoptosis was measured by determining the chromatin fragmentation in lung fibroblasts devoid of *cyt c* (clone LF-CL3) and fibroblasts with (KO19+COX10) or without (KO19) *COX10*, a factor necessary for COX assembly. We also analyzed LM(TK^-) cells with or without mtDNA ([rho^0]). $n = 4$; *, $P < 0.001$. Panel D shows the measurement of mitochondrial membrane potential by staining live cells with the fluorescent probe tetramethylrhodamine ethyl ester (TMRE) followed by flow cytometry. TNF-α–CHX treatment induces only a small decrease in the mitochondrial membrane potential, and this was not different for an OXPHOS-competent or -incompetent cell. Treatment of the cells with CCCP, a protonophore and uncoupler of oxidative phosphorylation, reduced the mitochondrial membrane potential in all the cells.

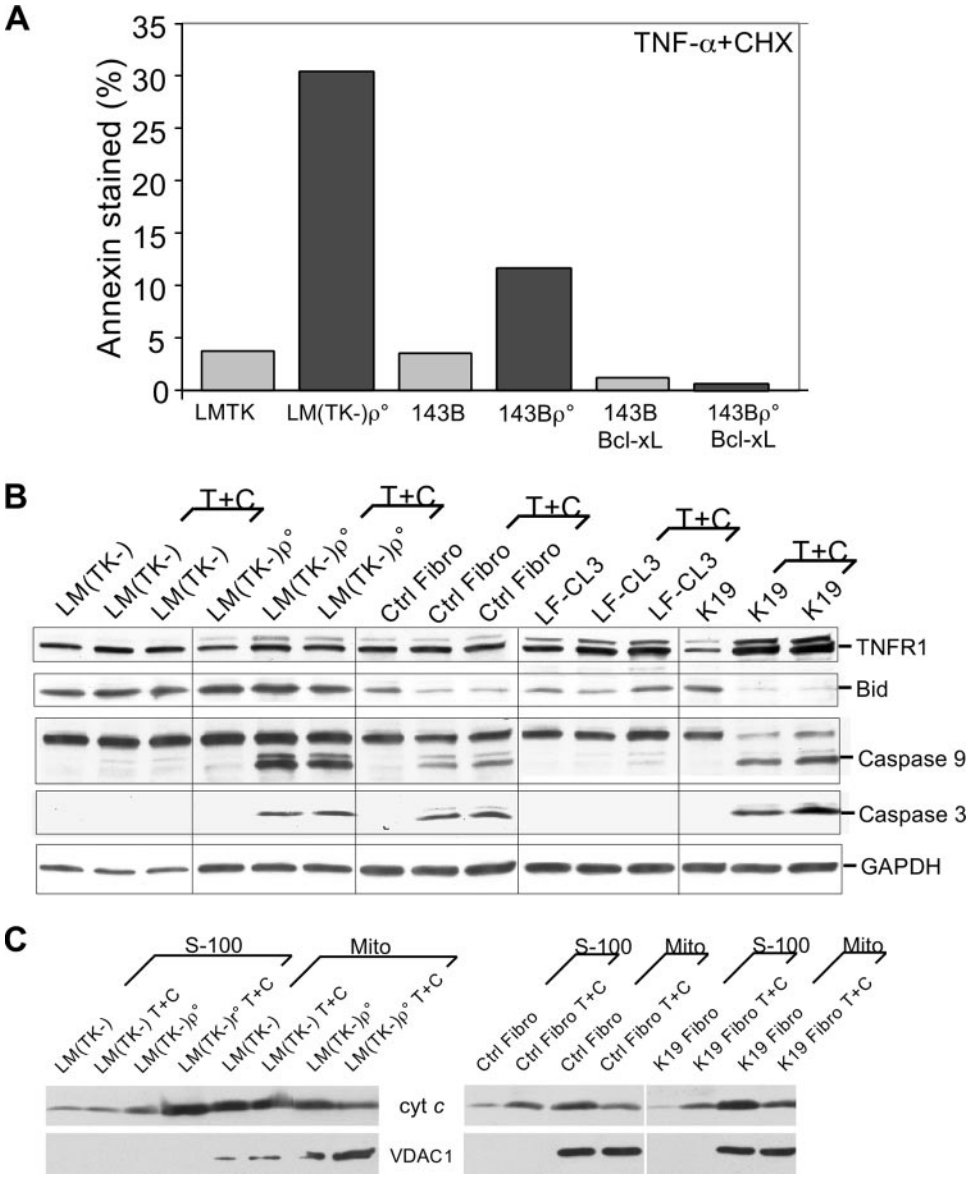

FIG. 9. Potential players in the increased TNF-α susceptibility of OXPHOS-deficient cells. Panel A, two cell lines and their mtDNA-less derivatives ([*rho*^{0}]) were treated with TNF-α plus CHX, and apoptosis was estimated by annexin V-FITC staining followed by flow cytometry. The human osteosarcoma cells (143B) and the mtDNA-less derivative overexpressing Bcl-xL were also analyzed. Panel B, Western blot analysis shows the steady-state levels of factors involved in the extrinsic apoptosis pathway after treatment with TNF-α plus CHX (T+C), including TNFR1, Bid, and caspase-3 and -9. Untreated cells were incubated with an equivalent amount of the DMSO solvent. tBid appeared as a weak band in Western blots. Therefore, we used the reduction in Bid as an estimate of its processing into tBid. Panel C shows the release of Cyt *c* from the mitochondria into the cytosol (S100 fraction) following treatment with TNF-α–CHX or DMSO.

staurosporine-induced apoptosis, even though the Cyt *c* mutant was more resistant. These findings indicate that the previous observation of TNF-α hypersensitivity in *cyt c* KO cells was related to decreased respiration and not to the lack of Cyt *c* release. We believe that changes in mitochondrial physiology are the culprit for this effect. After TNF-α treatment, there was an increase in the Western blot signal for TNFR1 in most cell lines analyzed. This is unlikely to be due to increased expression, since we used cycloheximide in the treatment. Therefore, it is more likely a consequence of other stabilizing events, such as reduced degradation or protection by endosomes. We did not observe great differences in Bid processing strictly correlating to OXPHOS-competent or -deficient cells. A recent study showed that cells deficient in cardiolipin have increased release of Cyt *c* and accelerated apoptosis (7). Interestingly, those authors also found that this phenotype was not associated with changes in tBid binding to mitochondria. COX10 KO fibroblasts have altered mitochondrial membrane structure compared to wild-type cells. The mitochondria are enlarged with abnormal cristae (11). Electron microscope studies of the *cyt c* double KO fibroblasts also revealed enlarged mitochondria with abnormal cristae (unpublished observations). It has

been proposed that architectural changes in the mitochondrial cristae are required for *cyt c* release during apoptosis (6, 31). Therefore, the membrane structure changes associated with cells lacking OXPHOS complexes may work in a similar fashion, potentiating apoptosis. We did observe a marked increase in Cyt *c* release in the LM(TK$^-$)ρ^0 cell line upon TNF-α–CHX treatment. A similar effect was also observed for the COX-deficient fibroblasts, but because this difference was not as striking as that for LM(TK$^-$)ρ^0, the relative importance of crista changes and Cyt *c* release for the increased sensitivity to TNF-α in OXPHOS-deficient cells requires further investigation.

In conclusion, this study showed that the testis isoform of Cyt *c* can be activated and promote apoptosis in somatic cells. The production of and investigations with a true *cyt c* null cell showed that Cyt *c* amplifies apoptosis triggered by TNF-α. Finally, this study also showed that hypersensitivity to TNF-α is associated with OXPHOS defects, likely due to changes in mitochondrial membranes and increased Cyt *c* release.

ACKNOWLEDGMENTS

We are grateful to Hirokazu Fukui for the *COX10* lentivirus construct, to Chandra Wozniak for assistance in performing the HPLC, and to the Transgene facility of the University of Miami for creating the *cyt c* transgenic mouse.

This work was supported by PHS grants R01-CA85700 and R01-NS41777 to C.T.M and R01-GM65813 to L.H.B. and by a postdoctoral Fellowship grant from the American Heart Association (FL/PR Affiliate) to U.D.V.

REFERENCES

1. **Algeciras-Schimnich, A., and M. E. Peter.** 2003. Actin dependent CD95 internalization is specific for Type I cells. FEBS Lett. **546:**185–188.
2. **Barrientos, A., L. Kenyon, and C. T. Moraes.** 1998. Human xenomitochondrial cybrids. Cellular models of mitochondrial complex I deficiency. J. Biol. Chem. **273:**14210–14217.
3. **Barrientos, A., D. Korr, and A. Tzagoloff.** 2002. Shy1p is necessary for full expression of mitochondrial COX1 in the yeast model of Leigh's syndrome. EMBO J. **21:**43–52.
4. **Buchet, K., and C. Godinot.** 1998. Functional F1-ATPase essential in maintaining growth and membrane potential of human mitochondrial DNA-depleted rho degrees cells. J. Biol. Chem. **273:**22983–22989.
5. **Cecconi, F., G. Alvarez-Bolado, B. I. Meyer, K. A. Roth, and P. Gruss.** 1998. Apaf1 (CED-4 homolog) regulates programmed cell death in mammalian development. Cell **94:**727–737.
6. **Cereghetti, G. M., and L. Scorrano.** 2006. The many shapes of mitochondrial death. Oncogene **25:**4717–4724.
7. **Choi, S. Y., F. Gonzalvez, G. M. Jenkins, C. Slomianny, D. Chretien, D. Arnoult, P. X. Petit, and M. A. Frohman.** 4 August 2006, posting date. Cardiolipin deficiency releases cytochrome c from the inner mitochondrial membrane and accelerates stimuli-elicited apoptosis. Cell Death Differ. [Epub ahead of print.]
8. **Crouser, E. D., M. E. Gadd, M. W. Julian, J. E. Huff, K. M. Broekemeier, K. A. Robbins, and D. R. Pfeiffer.** 2003. Quantitation of cytochrome c release from rat liver mitochondria. Anal. Biochem. **317:**67–75.
9. **Dey, R., A. Barrientos, and C. T. Moraes.** 2000. Functional constraints of nuclear-mitochondrial DNA interactions in xenomitochondrial rodent cell lines. J. Biol. Chem. **275:**31520–31527.
10. **Dey, R., and C. T. Moraes.** 2000. Lack of oxidative phosphorylation and low mitochondrial membrane potential decrease susceptibility to apoptosis and do not modulate the protective effect of Bcl-x(L) in osteosarcoma cells. J. Biol. Chem. **275:**7087–7094.
11. **Diaz, F., H. Fukui, S. Garcia, and C. T. Moraes.** 2006. Cytochrome *c* oxidase is required for the assembly/stability of respiratory complex I in mouse fibroblasts. Mol. Cell. Biol. **26:**4872–4881.
12. **Diaz, F., C. K. Thomas, S. Garcia, D. Hernandez, and C. T. Moraes.** 2005. Mice lacking COX10 in skeletal muscle recapitulate the phenotype of progressive mitochondrial myopathies associated with cytochrome c oxidase deficiency. Hum. Mol. Genet. **14:**2737–2748.
13. **Fumarola, C., and G. G. Guidotti.** 2004. Stress-induced apoptosis: toward a symmetry with receptor-mediated cell death. Apoptosis **9:**77–82.
14. **Gottlieb, R. A., and S. Adachi.** 2000. Nitrogen cavitation for cell disruption to obtain mitochondria from cultured cells. Methods Enzymol. **322:**213–221.
15. **Green, D. R.** 2005. Apoptotic pathways: ten minutes to dead. Cell **121:**671–674.
16. **Hakem, R., A. Hakem, G. S. Duncan, J. T. Henderson, M. Woo, M. S. Soengas, A. Elia, J. L. de la Pompa, D. Kagi, W. Khoo, J. Potter, R. Yoshida, S. A. Kaufman, S. W. Lowe, J. M. Penninger, and T. W. Mak.** 1998. Differential requirement for caspase 9 in apoptotic pathways in vivo. Cell **94:**339–352.
17. **Hao, Z., G. S. Duncan, C. C. Chang, A. Elia, M. Fang, A. Wakeham, H. Okada, T. Calzascia, Y. Jang, A. You-Ten, W. C. Yeh, P. Ohashi, X. Wang, and T. W. Mak.** 2005. Specific ablation of the apoptotic functions of cytochrome C reveals a differential requirement for cytochrome C and Apaf-1 in apoptosis. Cell **121:**579–591.
18. **Hess, R. A., L. A. Miller, J. D. Kirby, E. Margoliash, and E. Goldberg.** 1993. Immunoelectron microscopic localization of testicular and somatic cytochromes c in the seminiferous epithelium of the rat. Biol. Reprod. **48:**1299–1308.
19. **Hill, M. M., C. Adrain, P. J. Duriez, E. M. Creagh, and S. J. Martin.** 2004. Analysis of the composition, assembly kinetics and activity of native Apaf-1 apoptosomes. EMBO J. **23:**2134–2145.
20. **Jiang, X., and X. Wang.** 2004. Cytochrome C-mediated apoptosis. Annu. Rev. Biochem. **73:**87–106.
21. **Khosravi-Far, R., and M. D. Esposti.** 2004. Death receptor signals to mitochondria. Cancer Biol. Ther. **3:**1051–1057.
22. **Kluck, R. M., L. M. Ellerby, H. M. Ellerby, S. Naiem, M. P. Yaffe, E. Margoliash, D. Bredesen, A. G. Mauk, F. Sherman, and D. D. Newmeyer.** 2000. Determinants of cytochrome c pro-apoptotic activity. The role of lysine 72 trimethylation. J. Biol. Chem. **275:**16127–16133.
23. **Kuida, K., T. F. Haydar, C. Y. Kuan, Y. Gu, C. Taya, H. Karasuyama, M. S. Su, P. Rakic, and R. A. Flavell.** 1998. Reduced apoptosis and cytochrome c-mediated caspase activation in mice lacking caspase 9. Cell **94:**325–337.
24. **Lee, M. S., J. Y. Kim, and S. Y. Park.** 2004. Resistance of rho(0) cells against apoptosis. Ann. N. Y. Acad. Sci. **1011:**146–153.
25. **Li, H., H. Zhu, C. J. Xu, and J. Yuan.** 1998. Cleavage of BID by caspase 8 mediates the mitochondrial damage in the Fas pathway of apoptosis. Cell **94:**491–501.
26. **Li, K., Y. Li, J. M. Shelton, J. A. Richardson, E. Spencer, Z. J. Chen, X. Wang, and R. S. Williams.** 2000. Cytochrome c deficiency causes embryonic lethality and attenuates stress-induced apoptosis. Cell **101:**389–399.
27. **Li, P., D. Nijhawan, I. Budihardjo, S. M. Srinivasula, M. Ahmad, E. S. Alnemri, and X. Wang.** 1997. Cytochrome c and dATP-dependent formation of Apaf-1/caspase-9 complex initiates an apoptotic protease cascade. Cell **91:**479–489.
28. **Liu, X., C. N. Kim, J. Yang, R. Jemmerson, and X. Wang.** 1996. Induction of apoptotic program in cell-free extracts: requirement for dATP and cytochrome c. Cell **86:**147–157.
29. **Ludovico, P., F. Rodrigues, A. Almeida, M. T. Silva, A. Barrientos, and M. Corte-Real.** 2002. Cytochrome c release and mitochondria involvement in programmed cell death induced by acetic acid in Saccharomyces cerevisiae. Mol. Biol. Cell **13:**2598–2606.
30. **Luo, X., I. Budihardjo, H. Zou, C. Slaughter, and X. Wang.** 1998. Bid, a Bcl2 interacting protein, mediates cytochrome c release from mitochondria in response to activation of cell surface death receptors. Cell **94:**481–490.
31. **Martinou, J. C., and R. J. Youle.** 2006. Which came first, the cytochrome c release or the mitochondrial fission? Cell Death Differ. **13:**1291–1295.
32. **Nagata, S.** 1997. Apoptosis by death factor. Cell **88:**355–365.
33. **Narisawa, S., N. B. Hecht, E. Goldberg, K. M. Boatright, J. C. Reed, and J. L. Millan.** 2002. Testis-specific cytochrome *c*-null mice produce functional sperm but undergo early testicular atrophy. Mol. Cell. Biol. **22:**5554–5562.
34. **Park, S. Y., I. Chang, J. Y. Kim, S. W. Kang, S. H. Park, K. Singh, and M. S. Lee.** 2004. Resistance of mitochondrial DNA-depleted cells against cell death: role of mitochondrial superoxide dismutase. J. Biol. Chem. **279:**7512–7520.
35. **Picklo, M. J., J. Zhang, V. Q. Nguyen, D. G. Graham, and T. J. Montine.** 1999. High-pressure liquid chromatography quantitation of cytochrome c using 393 nm detection. Anal. Biochem. **276:**166–170.
36. **Read, S. H., B. C. Baliga, P. G. Ekert, D. L. Vaux, and S. Kumar.** 2002. A novel Apaf-1-independent putative caspase-2 activation complex. J. Cell Biol. **159:**739–745.
37. **Saelens, X., N. Festjens, L. Vande Walle, M. van Gurp, G. van Loo, and P. Vandenabeele.** 2004. Toxic proteins released from mitochondria in cell death. Oncogene **23:**2861–2874.
38. **Scaffidi, C., S. Fulda, A. Srinivasan, C. Friesen, F. Li, K. J. Tomaselli, K. M. Debatin, P. H. Krammer, and M. E. Peter.** 1998. Two CD95 (APO-1/Fas) signaling pathways. EMBO J. **17:**1675–1687.
39. **Slee, E. A., M. T. Harte, R. M. Kluck, B. B. Wolf, C. A. Casiano, D. D. Newmeyer, H. G. Wang, J. C. Reed, D. W. Nicholson, E. S. Alnemri, D. R. Green, and S. J. Martin.** 1999. Ordering the cytochrome c-initiated caspase cascade: hierarchical activation of caspases-2, -3, -6, -7, -8, and -10 in a caspase-9-dependent manner. J. Cell Biol. **144:**281–292.

40. **Sprick, M. R., and H. Walczak.** 2004. The interplay between the Bcl-2 family and death receptor-mediated apoptosis. Biochim. Biophys. Acta **1644:**125–132.
41. **Sun, X. M., S. B. Bratton, M. Butterworth, M. MacFarlane, and G. M. Cohen.** 2002. Bcl-2 and Bcl-xL inhibit CD95-mediated apoptosis by preventing mitochondrial release of Smac/DIABLO and subsequent inactivation of X-linked inhibitor-of-apoptosis protein. J. Biol. Chem. **277:** 11345–11351.
42. **Terradillos, O., S. Montessuit, D. C. Huang, and J. C. Martinou.** 2002. Direct addition of BimL to mitochondria does not lead to cytochrome c release. FEBS Lett. **522:**29–34.
43. **Twiddy, D., D. G. Brown, C. Adrain, R. Jukes, S. J. Martin, G. M. Cohen, M. MacFarlane, and K. Cain.** 2004. Pro-apoptotic proteins released from the mitochondria regulate the protein composition and caspase-processing activity of the native Apaf-1/caspase-9 apoptosome complex. J. Biol. Chem. **279:**19665–19682.
44. **Wei, M. C., W. X. Zong, E. H. Cheng, T. Lindsten, V. Panoutsakopoulou, A. J. Ross, K. A. Roth, G. R. MacGregor, C. B. Thompson, and S. J. Korsmeyer.** 2001. Proapoptotic BAX and BAK: a requisite gateway to mitochondrial dysfunction and death. Science **292:**727–730.
45. **Yoshida, H., Y. Y. Kong, R. Yoshida, A. J. Elia, A. Hakem, R. Hakem, J. M. Penninger, and T. W. Mak.** 1998. Apaf1 is required for mitochondrial pathways of apoptosis and brain development. Cell **94:**739–750.
46. **Zou, H., W. J. Henzel, X. Liu, A. Lutschg, and X. Wang.** 1997. Apaf-1, a human protein homologous to C. elegans CED-4, participates in cytochrome c-dependent activation of caspase-3. Cell **90:**405–413.